Ukrainian Journal of Ecology

*Ukrainian Journal of Ecology*, 2017, 7(4), 340–348, doi: 10.15421/2017_125

*ORIGINAL ARTICLE*

# Study on frequency content of provided strong ground motion in West Azerbaijan and East Azerbaijan

**Katayoun Behzadafshar**

*Department of Physics, College of Basic Sciences, Yadegar-e-Imam Khomeini (RAH) Shahre Rey Branch,Islamic Azad University, Tehran, Iran, E-mail: behzadafshar.k@gmail.com*

***Submitted: 31.10.2017. Accepted: 14.12.2017***

This study aims to better reveal the characteristics of the assessed ground motion in west and east Azerbaijan. Due to existence of happened great earthquakes and large number of potential seismic sources in North-West of Iran which is located in junction of Alborz and Zagros seismotectonic provinces, it is an interesting area for seismologists .Considering to population and existence of large cities like Tabriz, Ardabil and Orumiyeh which play crucial role in industry and economy of Iran, authors decided to focus on study of frequency content of strong ground motion to achieve ground acceleration in different frequencies indicate critical frequencies in the studied area. in this study have been applied is professional industrial software which has been written in 2009 and provided by authors; Because This applied software can cover previous software weak points very well. Obtained hazard maps illustrate that maximum accelerations will be experienced in North West to South East direction which increased by frequency reduction from 100 Hz to 10 Hz then decreased by frequency reduce (to 0.25 Hz). Maximum acceleration will be occurred in the basement in 10 Hz.

**Key words:** frequency; Earthquake; fault; professional industrial software

## Introduction

Probabilistic seismic hazard analysis (PSHA) is the most commonly used approach to evaluate the seismic parameters for the important engineering projects by which the rate of different ground motion levels in a selected site can be calculated. In a PSHA, effects of all the earthquakes are expected to occur at different locations are considered with associated uncertainties of earthquake occurrences and attenuation of seismic waves with distance. To analyze frequency effect on hazard maps a standard probabilistic procedure recommended by Cornell (1968) and McGuire (1976, 1978) is used.

This paper is an attempt to focus on the area with 44 E to 48 E latitude and 36 N to 39 N longitude which is located in Alborz – Azerbajjan seismotectonic province. North border of the province is located in south part of Caspian Sea where currently has low strain rate and its deformation behavior is different from the other parts of Iran (Jackson, 1992). Although from geological point of view, south border of the province is not obvious, considering Neoseismotectonic studies, it may be located on some active faults.

There is no significant geological line between the studied province and Kope Dagh province, so it has been determined by some seismic activities and the variety of geological formations. Continental shortening, due to the convergence of Arabian and Iran plates with a convergent rate of 30 mm/y (Jackson, 1992), is completed and compensated with continental crust thickening and lateral crust movement.

## Methodology

### Seismic potential sources

In PSHA method earthquakes' occurrence is assumed as a Poisson function, so events happen along faults or around potential sources randomly in time and space so the comprehensive knowledge of potential sources seems to be essential. The main recognized faults of this area can be listed as below.

The Tabriz fault (The North Tabriz fault): This fault significantly continues to Moro and Mishu Mountains (Nabavi, 1976) but due to lack of outcrops, its westward strike is somehow vague. North Tabriz fault's complexity (which is the result of a huge number of the fault's junctions) caused remarkable fault strike variations through the fault. The North Tabriz fault Strike between Tabriz and Sofian, is about N115 with vertical sleep in Berberian's opinion (1976).

The Orumiyeh fault: In Nabavi's opinion (1976) this fault is a part of the North Tabriz fault which continues from Maku to the south and has crossed east of Lake Orumiyeh and ends into the Zarineh- Rud River. The Salmas fault: Salmas fault caused the massive 1930 Salmas earthquake which destroyed Salamas city and all villages around it. This fault is located 90 km far from the Orumiyeh fault. The Soltaniyeh fault: This fault is parallel to Mount Soltaniyeh and located in the western border of the mountains. This fault strike is NW-SE with length of 50 km. The Tasuj fault: Tasuj is a quaternary fault with bended strike and 5 kilometers far from Tasuj city and Lake Orumiyeh. The North Mishu fault: In fact, the North Mishu fault is eastern continuation of the North Tabriz fault. The fault with several kilometers length is easily observed in Sofiyan to Marand Road in the south of Payam village and North of Mount Mishu. South Mishu fault: South Mishu fault with E –W strike and 61 kilometers length is located in south of Sarab in northern crest of Bozghush mountain. Fig 1 illustrates main faults with earthquake epicenters of last century.

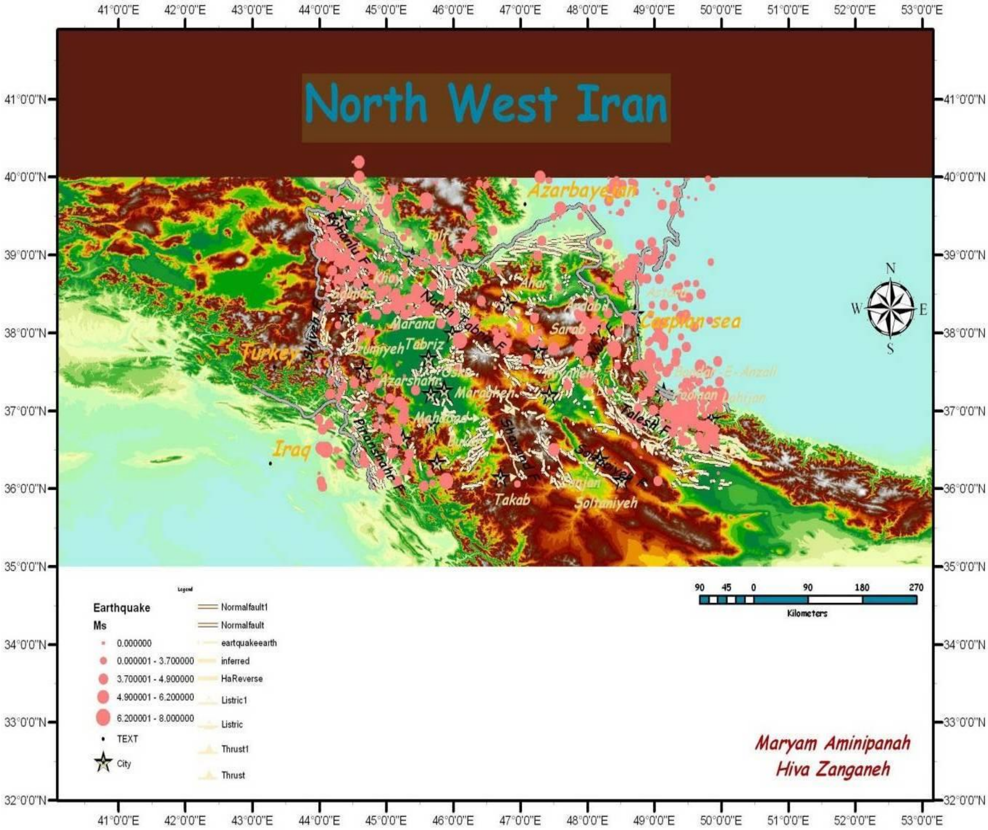


**Fig.1.** Main faults with earthquake epicenters of last century

Seismicity rate for both large and small earthquakes can be determined and taken into account for all potential sources by using special distribution function.

To achieve this purpose authors considered seismic database, seism tectonic and geological in formation (such as pale seismology results), studies on active structures (faults, folds, etc.) and stress pattern in the area.

In the present study in order to assess the proper special distribution function (SDF) four controlling factors has been considered as following:

Reliability of determined potential sources

Seism tectonic position of each potential sources

Structural elements of each seismic source

Seismicity features of each source

So 44 potential sources were given by Appling the conditions above.

Yen (1993) proposed a method to calculate SDF based on controlling factors for each magnitude, which is used in this paper.

In this method for each controlling factor (K) for each specified magnitude (j) in #l potential source distribution ratio, $W_{lmjk}$ was determined then the obtained distribution coefficient was normalized with the relationship bellow:

$$Q_{lmjk}= W_{lmjk}/\sum W_{lmjk} \quad (1)$$

In the next the total weight considering each source's controlling factor was determined by $R_{lmj}=\sum Q_{mjk}$

Finally, SDF was calculated by the equation bellow:

$$f_{l,mj}= R_{lmj}/\sum R_{lmj} \quad (2)$$

After all the obtained SDF in the studied area has been applied for the threshold magnitude of Ms=3 so weighted λ for each Kijko and Selevoll (1992) present a method to take into account magnitude uncertainty by threshold and maximum magnitude for different time intervals of complete catalogues to calculate seismic parameters, furthermore incomplete catalogue has been used in this method. In Kijko and Selevoll(1992) theory density distribution function and cumulative magnitude can be obtained by equation 5:

$$F(m \mid M) = \frac{\exp(-\beta_{M\min}) - \exp(-\beta m)}{\exp(-\beta M_{\min}) - \exp(-\beta M_{\max})} \quad (3)$$

Where:

m belongs to (Mmin, Mmax)

Provided Matlab code by authors (following Sharp 100 procedure) has been used to evaluate seismic activity parameters λ, β and Mmax. λ presents seismic activity rate and b or β(β=b Ln(10)) indicates number of large earthquakes to small ones ratio.

Considering equation 5 average annual occurrence rate for magnitude range of J for potential source number I was calculated from the following equation (Gao,1988)

$$\lambda_{I,mj} = \frac{2\lambda \exp[-\beta(m_j - M_{\min})] sh(.5\beta\Delta M)}{1 - \exp[-\beta(M_{\max} - M_{\min})]} f_{I,mj} \quad (4)$$

Whereas

$\lambda_{I,mj}$ shows the annual rate of occurrence and $f_{I,mj}$ represents spatial distribution function of magnitude # j in the #i potential source.

The authors' analysis provides an evidence to support the assumption in seismic hazard assessment that earthquakes are Poisson processes (Reiter 1990; Bozorgnia and Bertero 2004; Lombardi et al. 2005; Kossobokov 2006), which is routinely stated yet seldom tested or used as a constraint when fitting frequency-magnitude distributions. Therefore, Normal distribution function of probability which is described as following should be used in the study:

$$p(n) = \frac{(\lambda t)^n \exp(-\lambda t)}{n!} \quad (5)$$

Where:

$p(n)$ : Probability of occurrence for n earthquakes in duration of t

$\lambda$ : occurrence rate for earthquakes

So foreshocks and aftershocks which are taken into account as depended events cannot match with Poisson model and should be removed from the catalogue.

Among different represented time and spatial windows, Gardner and Knopoff (1974) windows have the most proper effect on removing dependent events in the studied area so the generated Matlab code by authors is used to apply the removal window in the present paper. In order to reach an independent catalogue 83.21% of earthquakes were determined as depended earthquakes and be removed from data base.

The independent catalogue belongs to a long-time interval which causes heterogeneity in time and space. Stepp's (1973) method has been applied to evaluate catalogue completeness. (eq. 2)

$$n = N / \Delta N \quad (6)$$

Where:

n: average rate of events

N: cumulative number of events

In this method calculated variance equals to $\sigma_n^2 = n/\Delta t$ and standard deviation, $\sigma_n$, is parallel to line $1/\sqrt{\Delta t}$

In the present paper Mirzaei et.al (2000) completeness diagram is taken into account to apply Stepp's method (fig2) .

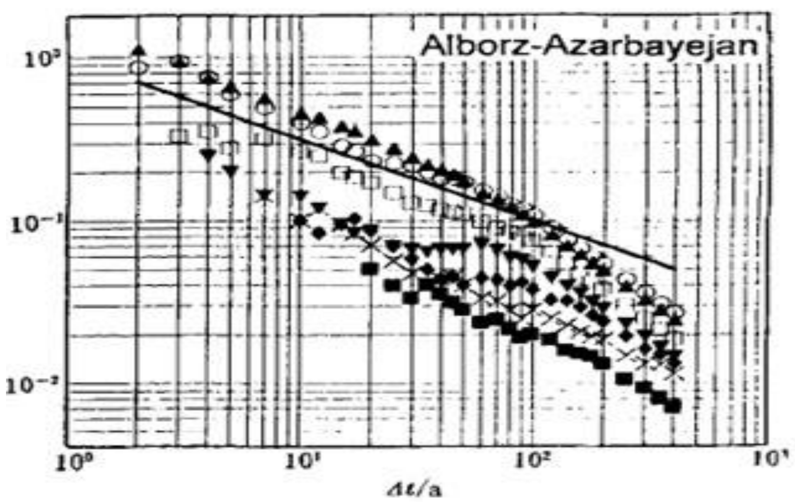


**Fig. 2.** Completeness evaluations in Alborz-Azerbaijan province (Mirzaii, 1997)

**Data base and data processing**

Instrumental earthquakes' catalogue just can cover recent events so return period estimation based on this catalogue can not guide us to the desired results. Therefore, historical earthquakes catalogue can play an important rule to determine more precise seismic activities. Historical document- based earthquakes in the studied area are listed in table 1. Time intervals without any seismic activity are signified in the table. Fig 3 illustrates special distribution and cumulative accumulation of occurrence.

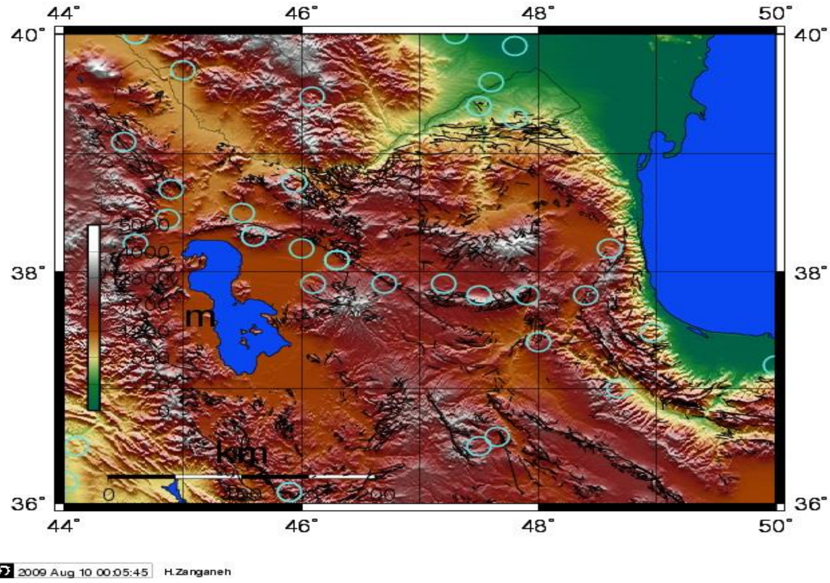


**Fig. 3.** Special distribution of historical events

**Table 1.** Historical earthquakes in the studied area

| | Year | month | Day | Hour | Latitude | Longitude | Depth | Mb | Ms | Mw |
|---|---|---|---|---|---|---|---|---|---|---|
| 1 | 735 | 0 | 0 | 0 | 39.7000 | 45.6000 | .0 | .0 | 6.5 | .0 |
| 2 | 858 | 0 | 0 | 0 | 38.1000 | 46.3000 | .0 | .0 | 6.0 | .0 |
| 3 | 863 | 2 | 13 | 0 | 40.0000 | 44.6000 | .0 | .0 | 5.2 | .0 |
| 4 | 893 | 12 | 24 | 0 | 40.0000 | 44.6000 | .0 | .0 | 6.0 | .0 |
| 5 | 906 | 4 | 1 | 0 | 39.7000 | 45.0000 | .0 | .0 | 6.1 | .0 |
| 6 | 1042 | 11 | 4 | 18 | 38.1000 | 46.3000 | .0 | .0 | 7.6 | .0 |
| 7 | 1135 | 7 | 25 | 0 | 36.1000 | 45.9000 | .0 | .0 | 6.1 | .0 |
| 8 | 1135 | 8 | 13 | 24 | 36.1000 | 45.9000 | .0 | .0 | 6.4 | .0 |
| 9 | 1179 | 4 | 29 | 18 | 36.5000 | 44.1000 | .0 | .0 | 6.6 | .0 |
| 10 | 1304 | 11 | 7 | 24 | 38.5000 | 45.5000 | .0 | .0 | 6.7 | .0 |
| 11 | 1319 | 1 | 1 | 0 | 39.1000 | 44.5000 | .0 | .0 | 5.3 | .0 |
| 12 | 1593 | 1 | 1 | 0 | 37.8000 | 47.5000 | .0 | .0 | 6.1 | .0 |
| 13 | 1641 | 2 | 5 | 18 | 37.9000 | 46.1000 | .0 | .0 | 6.8 | .0 |
| 14 | 1678 | 2 | 3 | 6 | 37.2000 | 50.0000 | .0 | .0 | 6.5 | .0 |
| 15 | 1717 | 3 | 12 | 6 | 38.1000 | 46.3000 | .0 | .0 | 5.9 | .0 |
| 16 | 1721 | 4 | 26 | 7 | 37.9000 | 46.7000 | .0 | .0 | 7.7 | .0 |
| 17 | 1780 | 1 | 8 | 24 | 38.2000 | 46.0000 | .0 | .0 | 7.7 | .0 |
| 18 | 1786 | 10 | 1 | 18 | 38.3000 | 45.6000 | .0 | .0 | 6.3 | .0 |
| 19 | 1843 | 4 | 18 | 8 | 38.7000 | 44.9000 | .0 | .0 | 5.9 | .0 |
| 20 | 1844 | 5 | 13 | 19 | 37.4000 | 48.0000 | .0 | .0 | 6.9 | .0 |
| 21 | 1851 | 4 | 9 | 16 | 40.0000 | 47.3000 | .0 | .0 | 6.2 | .0 |
| 22 | 1861 | 5 | 24 | 16 | 39.4000 | 47.5000 | .0 | .0 | 6.0 | .0 |
| 23 | 1862 | 12 | 19 | 5 | 39.3000 | 47.8000 | .0 | .0 | 6.1 | .0 |
| 24 | 1863 | 12 | 30 | 22 | 38.2000 | 48.6000 | .0 | .0 | 6.1 | .0 |
| 25 | 1868 | 3 | 18 | 17 | 39.6000 | 47.6000 | .0 | .0 | 6.0 | .0 |
| 26 | 1876 | 10 | 1 | 0 | 38.3000 | 45.6000 | .0 | .0 | 6.3 | .0 |
| 27 | 1879 | 3 | 22 | 4 | 37.8000 | 47.9000 | .0 | .0 | 6.7 | .0 |
| 28 | 1880 | 7 | 4 | 0 | 36.5000 | 47.5000 | .0 | .0 | 5.6 | .0 |
| 29 | 1883 | 5 | 3 | 12 | 37.9000 | 47.2000 | .0 | .0 | 6.2 | .0 |
| 30 | 1896 | 1 | 4 | 16 | 37.8000 | 48.4000 | .0 | .0 | 6.7 | .0 |

The instrumental records were collected from several open sources such as National Geo database of Iran (www.ngdir.ir); Building and Housing Research Center (www.bhrc.ac.ir); USGS (www.usgs.gov), and ISC (www.ISC.UK).

Although Iran's instrumental recording started at the end of19$^{th}$ century with European seismograms, number of well-equipped stations have been developed after 1963.

Considering fig 4, events in the studied area are divided into three time intervals (1860- 1900, 1900-1975 and 1975-2016). Studies show that Alborz-Azerbajjan province includes the most completeness in recorded data among other provinces in Iran which can be the consequence of Karnik (1969) studies in his area.
Variation of cumulative number of events from 1900 to 2016 in Fig 4 confirms using separate time intervals in seismicity studies.

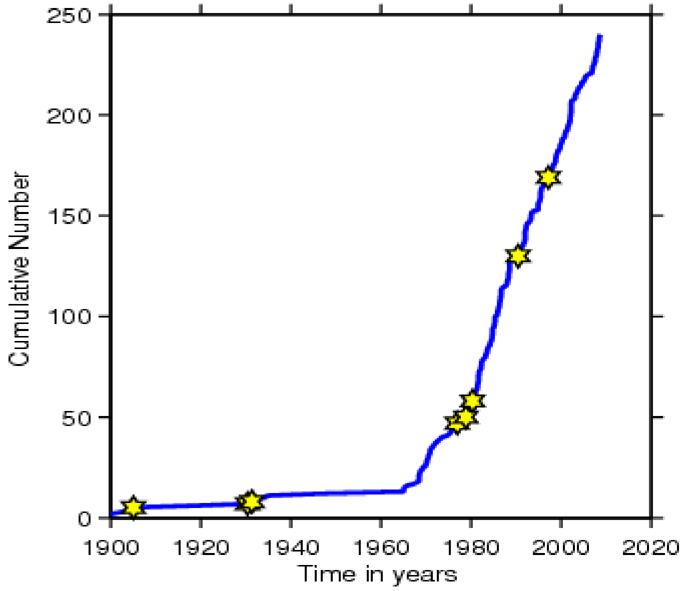


**Fig. 4.** Cumulative accumulation of events by time (1900-2016)

Comparison between the annual rate of events in two time intervals 1900-1963 and 1964-2016 in Fig 5 demonstrates a significant increase of reports after ISC installation which is more attentive for small earthquakes.

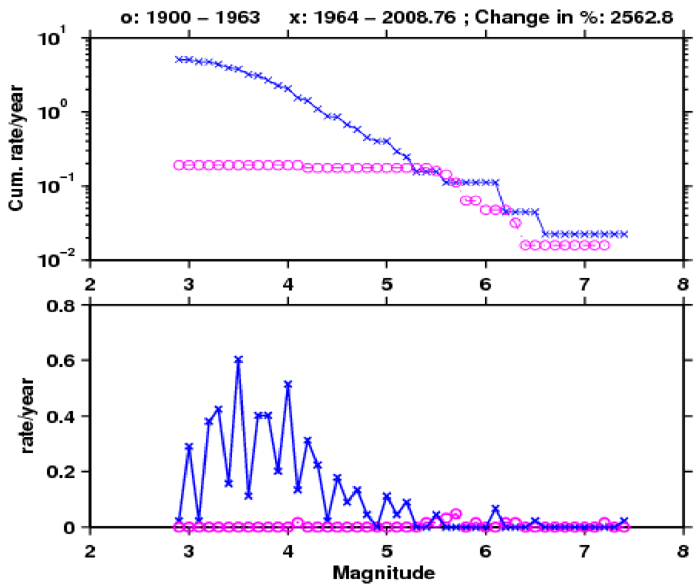


**Fig. 5.** Annual rate of events in two time intervals:1900-1963 (pink line) and 1964-2011 (blue line) (cumulative and noncumulative)

## Results ad Discussion

**Frequency analysis:**
Choosing an appropriate attenuation relationship is very important, and therefore, some general rules should be paid attention on to select a proper attenuation model.
1. The standard deviation of the regression result should be as small as possible.
2. The attenuation model itself has physical and practical backgrounds.
3. The predicted results could be applied to the areas which are lack of strong ground motion data, which indicates the popularity and applicability of the attenuation model (Esmailabadi, 2014)
Based on these rules, some attenuation models are proposed by different researchers can be applied to create iso-acceleration maps.In the present study, at first proposed attenuation relationships by Ambraseys et al. (1996) have been applied but the results showed according to 2800 building code there is an overestimation trend in using these relationships so in the second try Campbell and Bozorgnia (2003) attenuation relationships has been used to achieve isoacceleration maps for different frequency contents in 475 years recurrence interval with10% occurrence probability in 0.01, 0.05, 0.1,0.2, 0.5, 1, 2, and 4 s.

Results for frequency contents of 100 Hz (PGA), 20 Hz, 10 Hz , 1Hz ,0.5Hz and 0.25Hz has been illustrated in Figures 6,7,8,9,10,11 and12.

On base of Fig. 6, maximum PGA (0.0053 g) will be experienced in a NW-SE strike which fitted well with North Tabriz fault. It matches with the expected trend influenced by tectonic evidences and statistical studies. In 20 Hz frequency, maximum acceleration up to 0.0101g will be occurred in Tabriz area (Fig 7), but in frequency of 10 Hz, maximum hazard will happen in North Tabriz fault strike also west of Ardabil city (Fig 8). As Fig 9 shows north east of North Tabriz fault will be experienced maximum acceleration of .0364 in 2 Hz. Isoacceleration map (Fig 10) indicates in frequency of 1 Hz acceleration in the area with longitude of 45.00 to 45.50 E and latitude of 38.50 to 39.00 N will be the maximum among other frequency contents with the amount of 0.0447g whereas the minimum acceleration counter belongs to the area in north of Ardabil with 0.00155g. Fig 11 and 12 indicate maximum acceleration will be occurred in northwest corner of the studied area with acceleration of .04103 and 03474 for frequency contents of .5 Hz and .25 Hz respectively.

At last, a diagram which is indicating the relation between ground acceleration and frequency for the area was provided and presented in Fig 13. This obtained diagram shows the frequency content affects on predicted ground acceleration in the studied area.

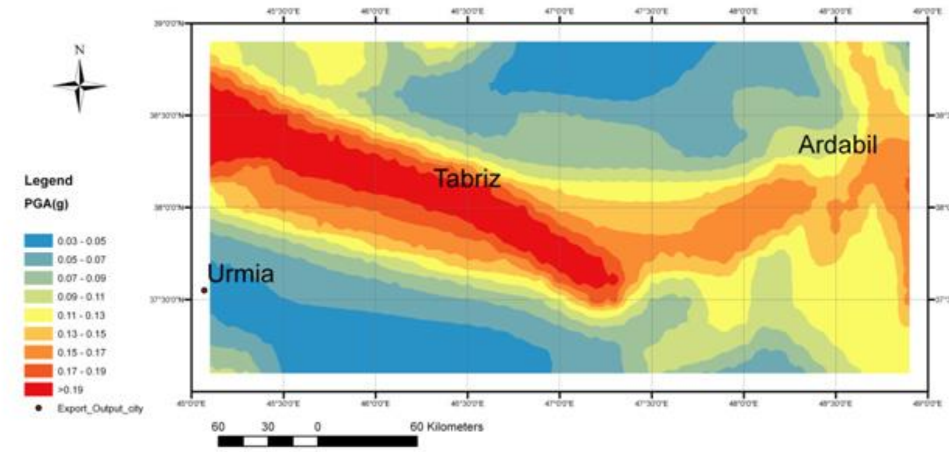


**Fig. 6.** Peak ground acceleration for 10% occurrence probability

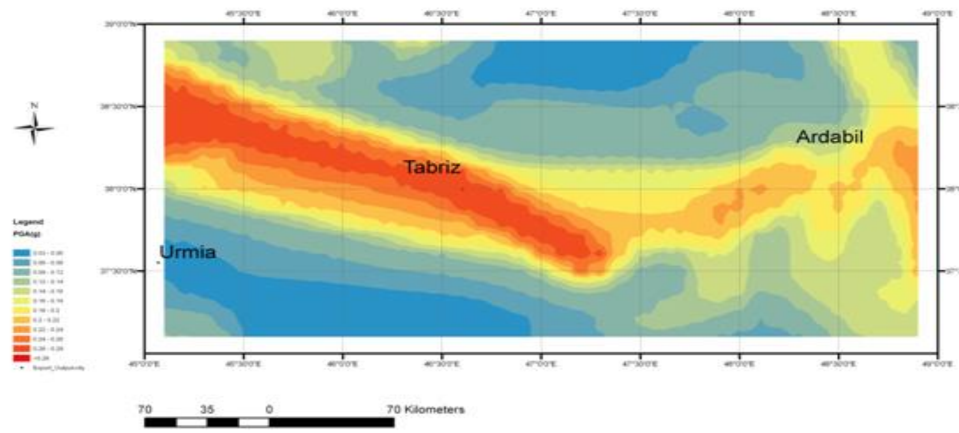


**Fig. 7.** Ground acceleration in 20Hz for 10% occurrence probability

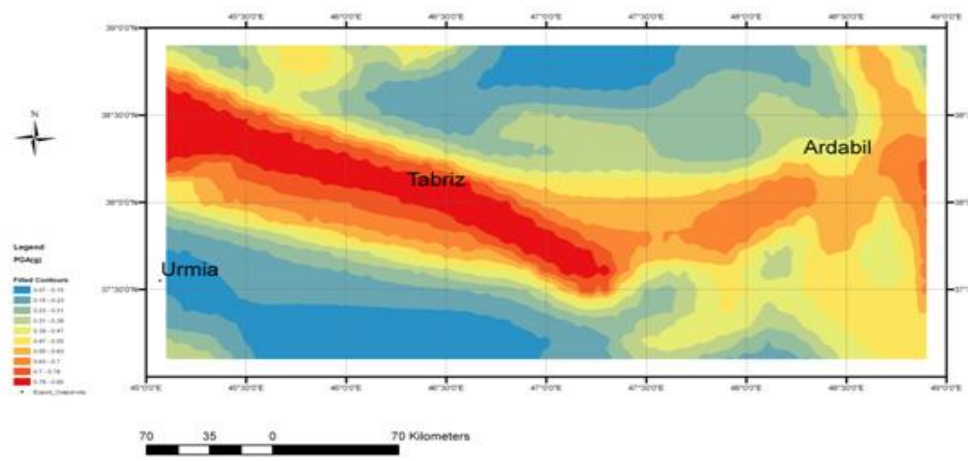


**Fig. 8.** Ground acceleration in 10 Hz for10% occurrence probability

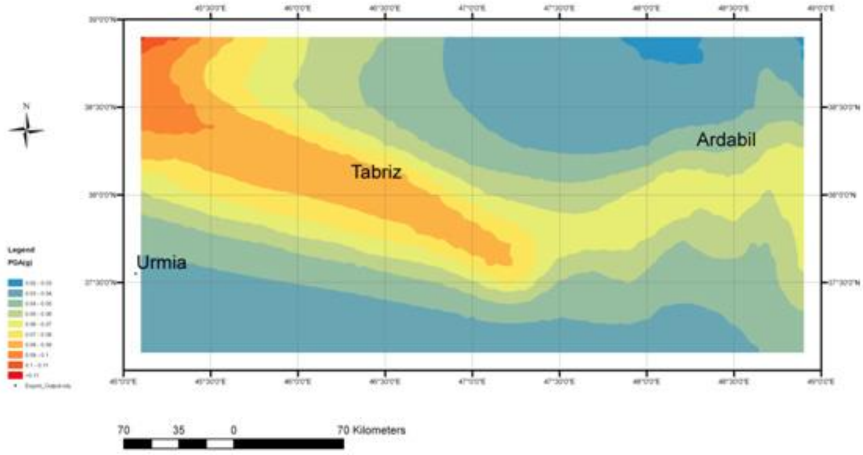


**Fig. 9.** Ground acceleration in 2 Hz for 10% occurrence probability

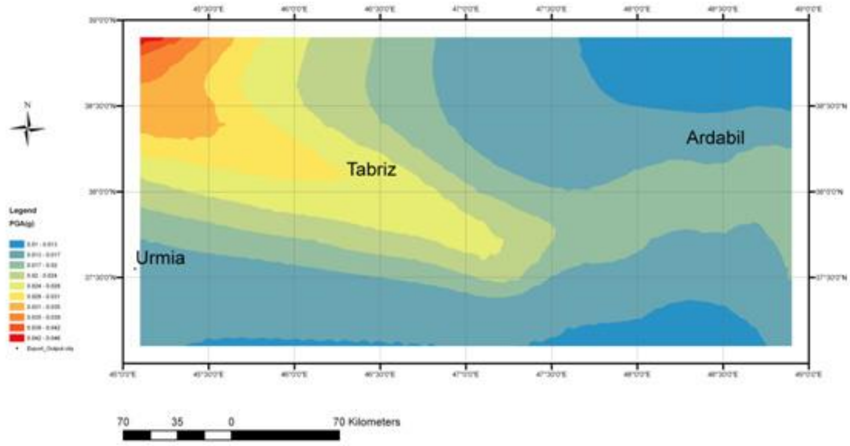


**Fig. 10.** Ground acceleration in 1 Hz for 10% occurrence probability

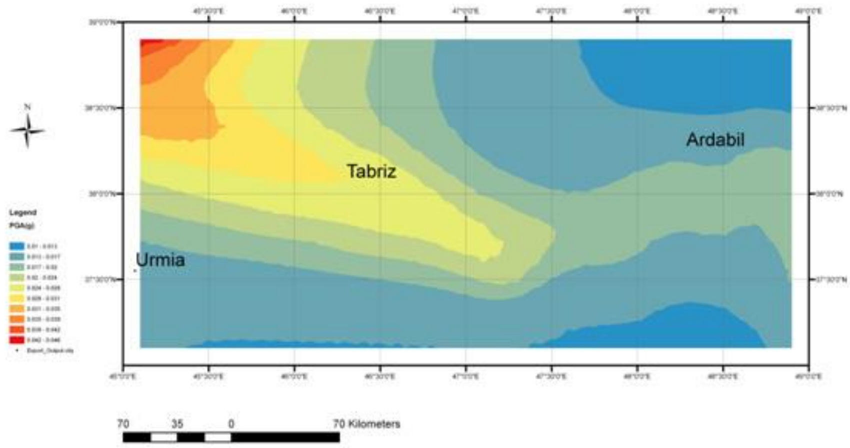


**Fig. 11.** Ground acceleration in 0.5Hz for 10% occurrence probability

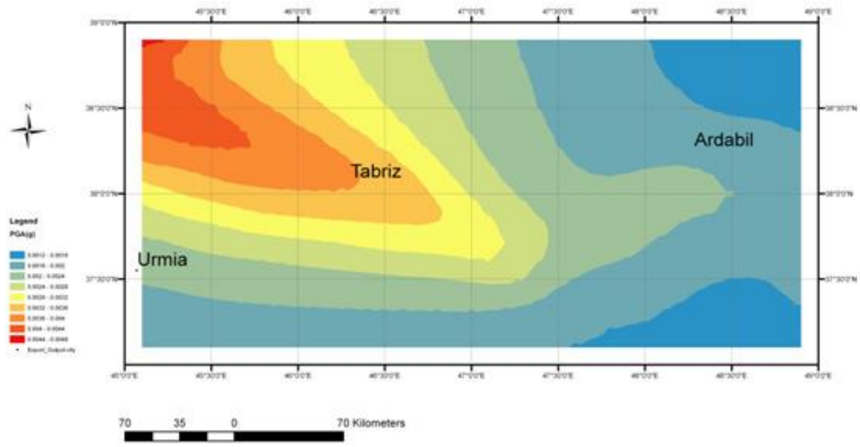


**Fig. 12.** Ground acceleration in 0.25 Hz for 10% occurrence probability

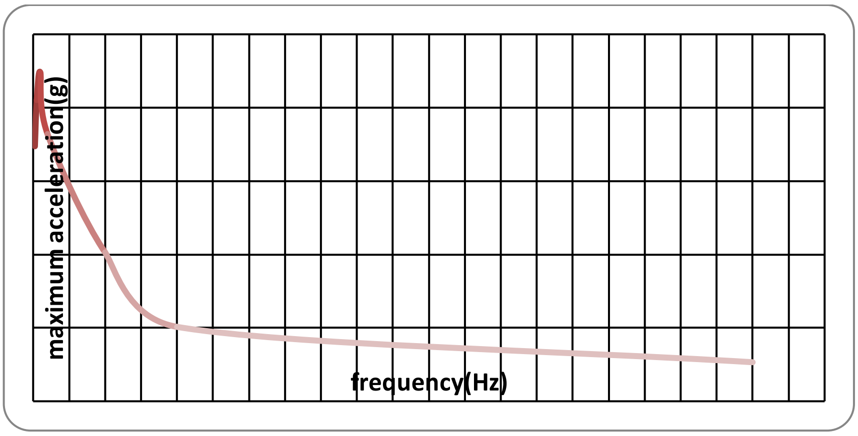


**Fig. 13.** Variation of maximum ground acceleration vs. frequency content

Fig13 shows the variation of acceleration by frequency, correlations between the considered parameters were determined for the entire frequency set in an acceptable frequency bandwidth. It describes a significant increasing trend for ground acceleration through the frequency content from 0.25 to 2Hz, the raising trend continues in slight way from 2 Hz to 10Hz in which the diagram reached the peak. Then an exponential decreasing trend from 10 to 100 Hz is obvious in the diagram.

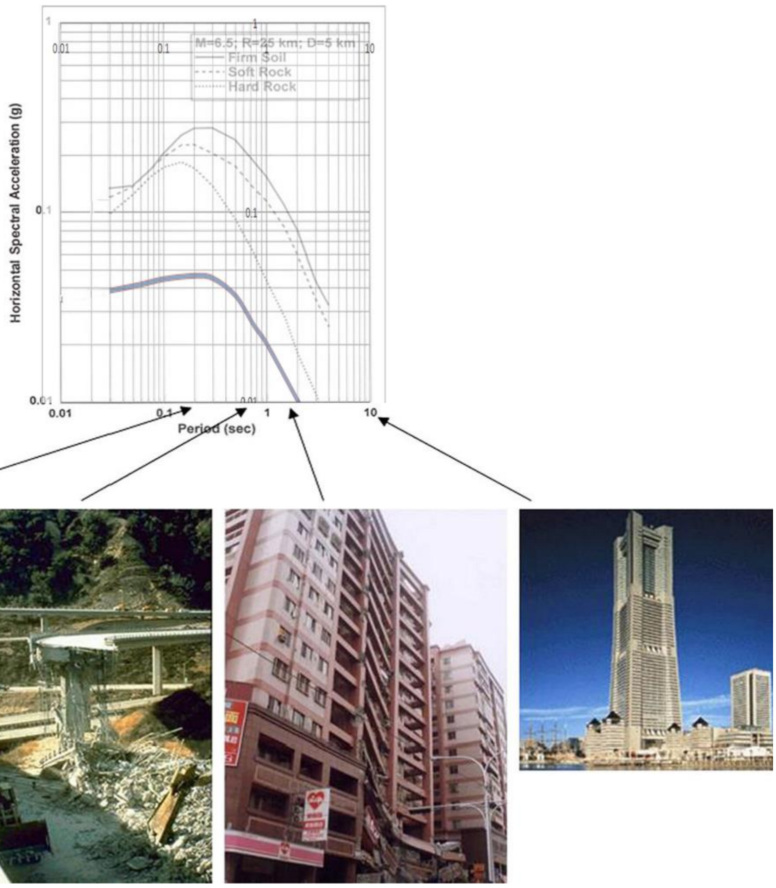


**Fig. 14.** Compared spectral Acceleration variation vs period between the present literature and the previous study

## Conclusion

The frequency content of an earthquake ground motion is important because it affects the dynamic response of earth and structural systems. It is also useful in earthquake engineering practice to characterize the frequency content of an earthquake ground motion with a single parameter such as ground acceleration, ground velocity, etc. Probabilistic method used in this literature, to describe the frequency content of the ground acceleration in the studied area.

Fig 14 were found to be the characteristics period based on modified definition of the effective peak ground motion values. The thick line indicates the obtained result, comparing with the presented diagram the achieved one in this article shows the increase of ground acceleration in lower periods whereas it's correlation with frequency content of small and moderate earthquakes can explain overestimate damages among these events the diagram reached the peak at T=0.1 s which is slightly more than the previous study, afterwards the same trend in decreasing ground acceleration is obvious which can reduce losses and damages in maintained frequency domain, Respect to the fact that each level of building can increase natural period of the structure about 0.1 s more so the diagram can suggest the most vulnerable building codes. Further studies will be needed to clarify the dependency of the frequency content of the analyzed motions on different factors such as slip distribution function, directivity effect and site conditions.

## References

Ambraseys, N., Simpson, K., Bommer, J. (1996). Prediction of horizontalresponse spectra in Europe. J Earthq Eng Struct Dyn, 25(4), 371–400.
Berberian, M. (1976). Active faulting and tectonics of Iran, in Zagros, Hindu Kush, Himalaya geodynamic evolution. In: Gupta HK, Delany FM (Eds.) Geodyn Ser Am Geophys Un, 3, 33–69.
Bozorgnia, Y., Bertero, V.V. (2004). Earthquake engineering: from engineering seismology to performance-based engineering. CRC Press, Boca Raton.
Cornell, C.A. (1968). Engineering seismic risk analysis. Bull Seismol Soc Am, 58, 1583–1606.
Esmailabadi, R., Abbaszadeh Shahri, A., Behzadafshar, K., Gheirati, A., Nosrati, J. (2014). Frequency content analysis of the probable earthquake in Kopeh Dagh region (Northeast of Iran). Arabian Journal of Geosciences, 11, 41-65.
Gao, M. (1988). Discussion on annual occurrence rates., Dev World Seismol, 1, 1–5 (in Chinese).
Gardner, J., Knopoff, K. (1974). Is the sequence of earthquakes in Southern California, with aftershock remove Poissonian? Bull Seismol Soc Am, 64, 1363–1367.
Jackson, J. (1992). Partitioning of strike-slip and convergent motion between Eurasia and Arabia in eastern Turkey and the Caucasus. J. geophys. Res., 97(12), 471-812.
Karnik, V. (1969). Seismicity of the European area. Part1. D. Reidel Pub.CO, Dordecht-Holland.
Kijko, A., Sellevoll, M.A. (1992). Estimation of earthquake hazard parameters from incomplete data files. Part II. Incorporating magnitude heterogeneity. Bull Seismol Soc Am, 82, 120–134.
Kossobokov, V.G. (2006). Testing earthquake predictionmethods: the West Pacific short-term forecast of earthquakes with magnitude MwHRV>=5.8. Tectonophysics, 413, 25–31.
Lombardi, A.M., Akinci, A., Malagnini, L., Mueller, C.S. (2005). Uncertainty analysis for seismic hazard in Northern and Central Italy. Ann Geophys, 48, 853–865.
McGuire, R.K. (1967). FORTRAN computer program for seismic risk analysis. US Geol Surv, Open File Rep, 76–67.
McGuire, R.K. (1978). FRISK—a computer program for seismic risk analysis. US Department of Interior. Geol Surv Open File Rep, 78–1007.
Mirzaei, N. (1997). Seismic zoning of Iran. PhD dissertation, Institute of Geophysics. State Seismological Bureau, Beijing.
Mirzaei, N., Kazemian, J., Karkuti, E., Shabani, E. (2000). Seisrisk iii+ manual. Geophysic Institute of Tehran University.
Nabavi, M.J. (1976). An introduction to geology. NGDIR. press, Tehran, Iran.
Reiter, L. (1990). Earthquake hazard analysis: issues and insights. Columbia University. Press, New York.
Stepp, J.C. (1973). Analysis of completeness of the earthquake sample in the Puget Sound area. In: Contribution to seismic zoning, NOAA Tech, Report, ERL 267-ESL30. Washington, D.C.

***Citation:***
Katayoun Behzadafshar (2017). Study on frequency content of provided strong ground motion in West Azerbaijan and East Azerbaijan. *Ukrainian Journal of Ecology, 7*(4), 340–348